

## CHAPTER 32

### WAVE TRANSFORMATIONS OVER A SUBMERGED BAR: EXPERIMENTS AND THEORETICAL INTERPRETATIONS

Gianfranco Liberatore<sup>1</sup> and Marco Petti<sup>2</sup>

#### Abstract

Random wave tests were performed in a flume to investigate wave transformations above a submerged bar built on a horizontal bottom.

Wave data were analysed in the frequency and time domains. In the time domain, reference was made both to short ( $f > 0.5f_p$ ) and long waves (with  $f < 0.5f_p$ ). This allowed in particular investigation of transformations of long waves passing over the bar.

Experimental results were interpreted using a second-order analytical model, able to separate first- and second-order components from given (measured) variance spectra. The analytical method proved to be conveniently applicable as long as breaking phenomena are not too intense.

#### Introduction

As is well-known, the presence of a bar in domains of relatively shallow-water severely modifies the evolution of wave trains during their propagation from deep to shallow water.

At present, knowledge of wave transformations over submerged bars is not satisfactory and theoretical models are still not able to take into account adequately phenomena such as wave breaking occurring on a bar in shallow waters. The problem, certainly interesting from both the theoretical and engineering points of view, has recently been studied in several theoretical investigations aiming at a better mathematical description of wave transformations over a bar. In this regard, recent theoretical contributions deal, for example, with inclusion of breaking effects in Boussinesq-type equations (e.g., Schäffer et al., 1991, Brocchini et al., 1991) or in mild slope type equations (Rojanakamthorn et al. 1989). A number of experimental

---

<sup>1</sup>Associate Professor, Institute of Maritime Structures, University of Padova, Via Ognissanti, 39 – 35129 Padova (Italy)

<sup>2</sup>Researcher, Department of Civil Engineering, University of Firenze, Via S. Marta, 3 – 50139 Firenze (Italy)

investigations has also been conducted recently to improve understanding of wave transformations over bars and to calibrate numerical models (Thorkilsen et al., 1991, Liberatore and Petti, 1991, Battjes and Beji, 1992, Beji et al., 1992, Smith and Kraus, 1992).

The aim of the present paper is first to contribute via experimental investigations to better understanding of the phenomena occurring when a bar is present and, second, to interpret spectral transformations using a non-linear (second-order) theoretical model (Petti, 1991).

### Experimental apparatus and procedure

Investigations were carried out in a flume 33 m long, 1 m wide and 1.2 m deep. A smooth 30 cm high submerged bar, with offshore slope 1:20, inshore slope 1:10 and top width of 2 m was built on the horizontal (concrete) bottom of the flume. A spending beach with slope 1:10 (covered with absorbing mattresses) was also modelled in the flume (Fig. 1). Concrete was used to built both bar and beach.

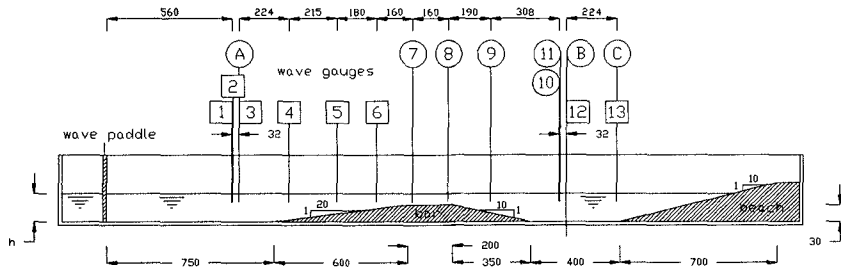


Fig.1 – *Experimental apparatus and location of wave gauges*

Waves were measured at thirteen measuring stations in the flume using eight parallel wire resistance wave gauges in two shifts. In Fig. 1, squared numbers correspond to group 1 (8 gauges, first shift) and circled numbers and letters to group 2 (second shift). Three of the measuring points (A, B and C) were common to the two shifts, enabling the repeatability of the two experiments to be checked. The gauges were set up so as to permit measurement of transformations of waves passing the bar, as well as reflections from both bar and spending beach.

Two offshore water depths of 40 and 50 cm were considered in the experiments; water depth above the bar was therefore 10 and 20 cm respectively.

For each water depth, three different random wave trains were generated. Their characteristics are shown in Tab.1.

Waves in the flume were produced by an hydraulically driven servo-controlled wave generator operated by a personal computer. A white noise filtering technique was used for wave generation. Every run lasted 1000 s. Sampling rate was 10 Hz.

Both short and long waves were analysed by filtering the signal and, considering the frequencies respectively higher and lower than  $0.5f_p$ , reconstructing the time domain signal (the basis for subsequent zero-crossing

analyses) using Inverse Fourier Transforms. This type of procedure was first proposed by Petti (1988).

Table 1 – *Characteristics of waves generated in flume.*

| Test no. | $\alpha$ | $f_p$ (Hz) | $H_{m_0}$ (cm) | $\gamma$ | depth (cm) |
|----------|----------|------------|----------------|----------|------------|
| 1        | 0.0075   | 0.650      | 9.8            | 2.0      | 40         |
| 2        | 0.0081   | 0.781      | 7.9            | 3.0      | 40         |
| 3        | 0.0081   | 0.850      | 7.0            | 3.0      | 40         |
| 4        | 0.0075   | 0.650      | 11.6           | 2.0      | 50         |
| 5        | 0.0075   | 0.781      | 9.4            | 3.0      | 50         |
| 6        | 0.0081   | 0.850      | 8.2            | 3.0      | 50         |

Reflection coefficients in front of the bar and in front of the spending beach were also calculated using the method of Goda and Suzuki (1976).

For short waves, these coefficients ranged between 0.17 and 0.22 for the berm, and between 0.22 and 0.30 for the beach (lower values corresponding to shorter peak periods). For long waves, reflection coefficients were much higher, varying between 0.91 and 0.98 for the bar and between 0.62 and 0.70 for the beach.

### Results of experiments

As an example, Figs. 3a and 3b show profiles of short and long waves in the time domain obtained for gauges 1 and 6 during test 1. As the figures show, non-linearities and consequent long waves are definitely more pronounced for gauge 6, located at a shallower depth.

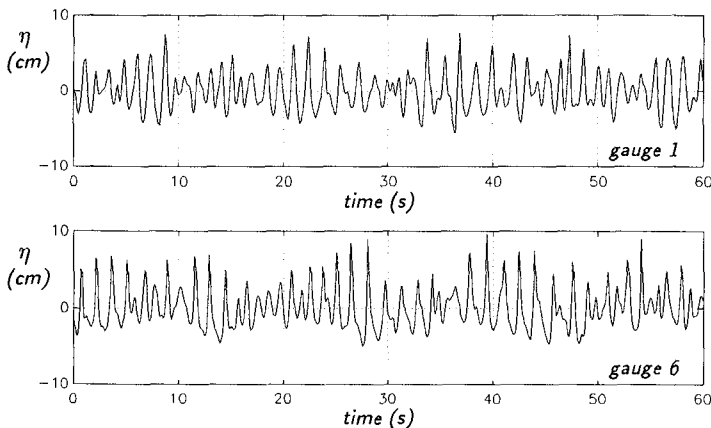


Fig. 3a – *Example of profiles of short waves in time domain (test 1).*

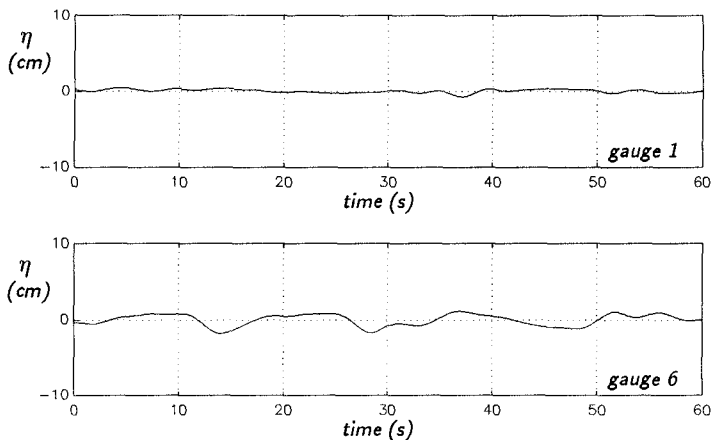


Fig. 3b – Example of profiles of long waves in time domain (test 1).

Spectral analyses generally reveal non-linear transformations of spectra on the seaside slope of the bar, with build-up of energy at low and high frequencies ( $f=2f_p$ ) due to shallow water effects. As a consequence of wave breaking processes on the bar, further transformations of spectra occur, leading to decreased energy depending on intensity of breaking. Behind the bar, rather broad, uniform spectra result.

Wave spectra computed during test 1 ( $h=40$  cm,  $f_p=0.65$  Hz,  $H_{m0}=9.8$  cm) are shown as examples in Figs. 4a and 4b.

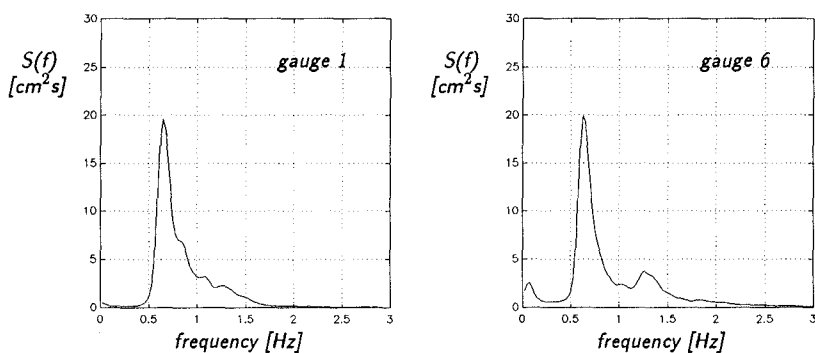


Fig.4a – Wave spectra obtained for test 1 (gauges 1 and 6).

Figs. 5 and 6 show trends for significant short wave heights  $H_s$  and for corresponding periods  $T_s$ , obtained for the two water depths of 40 and 50 cm, for all random wave trains generated during the experiments.

Figs. 5a show some increases in wave heights in the wave trains considered, due to shoaling effects, reaching a maximum on the seaside slope of the bar.

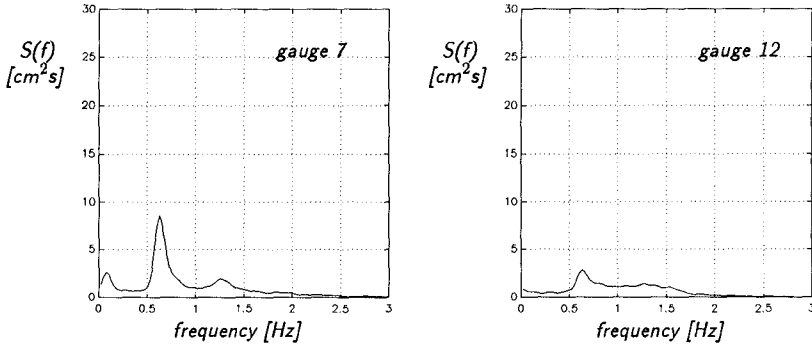


Fig.4b – Wave spectra obtained for test 1 (gauges 7 and 12)

Then decreases occur, due to breaking effects for waves passing the bar, with (nearly) constant wave heights for the three wave trains considered here.

Similar trends are observed for the greater water depth (50 cm; Fig. 6a), although in this case breaking processes are weaker and decreases in wave height are also less evident.

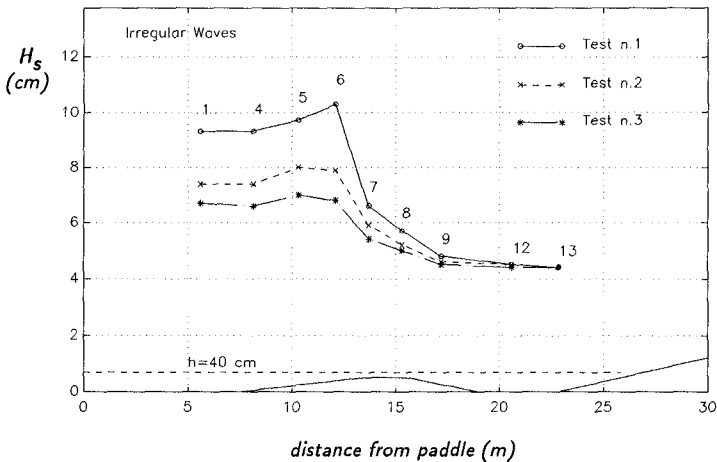


Fig. 5a – Significant wave heights of short waves calculated along flume for tests 1 – 3.

As regards wave periods, in the case of the 40 cm depth (Fig. 5b), after slight, rather uniform increases up to the top of the bar, decreases occur after the bar, and these are probably related to the intensity of breaking.

For the 50 cm water depth (Fig. 6b), periods are quite uniform with slight increases in the area of the bar.

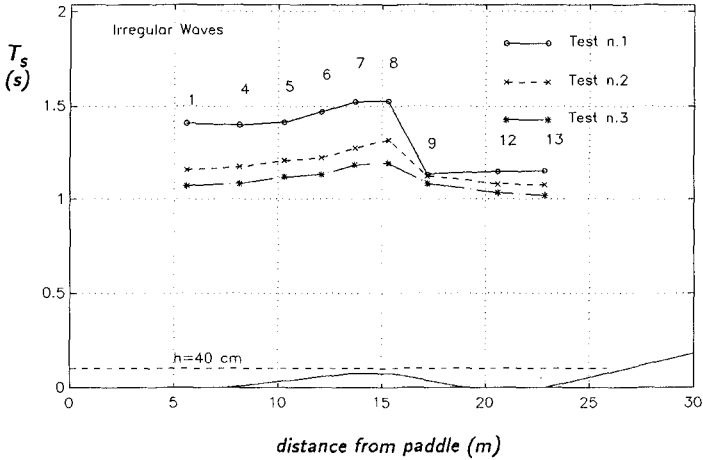


Fig. 5b—Significant periods of short waves calculated along flume for tests 1–3.

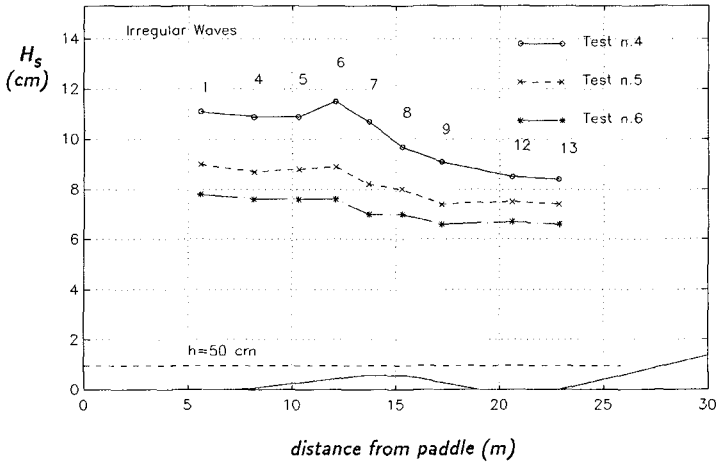


Fig. 6a—Significant heights of short waves calculated along flume for tests 4–6.

As regards long waves (Figs. 7a and 7b), in the case of the 40 cm water depth, their significant wave height initially increases, reaching a maximum on the top of the bar. After that, they rapidly decrease, although their height is still higher than offshore the bar.

This effect might at first sight be ascribed to flume seiches: this, however, would not explain wave height asymmetries with respect to the bar.

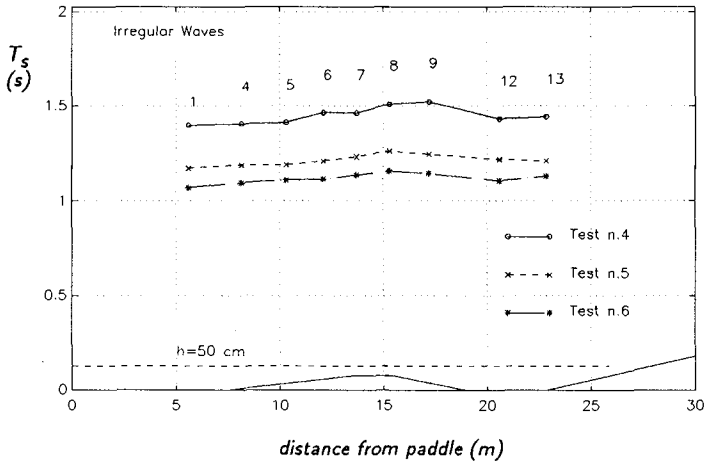


Fig. 6b—Significant periods of short waves calculated along flume for tests 4–6.

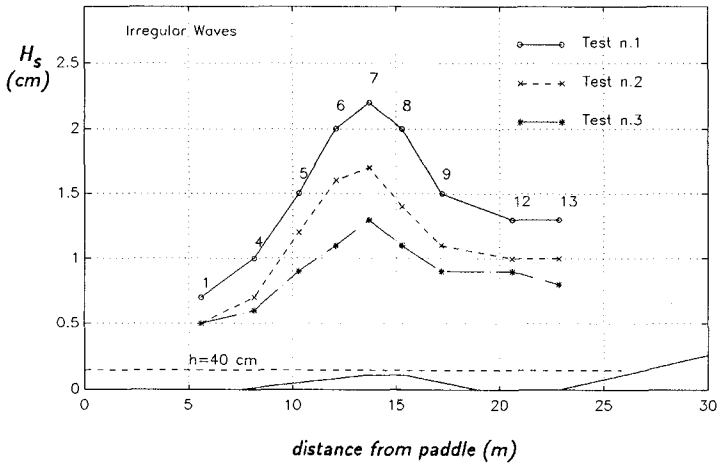


Fig. 7a—Significant heights of long waves calculated along flume for tests 1–3.

Instead, in our opinion, this phenomenon may more probably be ascribed either to seiches occurring between the bar and the spending beach or to partial persistence of the long waves generated above the bar.

Similar trends are also observed for the greater water depth (50 cm), although in this case breaking processes are weaker and decreases also less evident (Fig. 7b).

The significant periods of long wave ranged between 8 and 12 s.

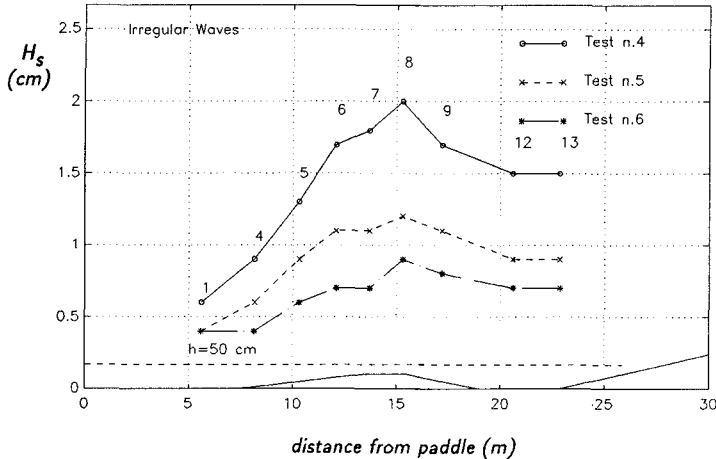


Fig. 7b – Significant heights of long waves calculated along flume for tests 4 – 6.

### Resumé of theoretical model

A non-linear theoretical model, able to separate first and second order components from a given non-linear (measured) spectrum, was utilised to interpret the experimental data. The model (Petti, 1991), is based on a systemic approach to sea wave behaviour and on some characteristic parameters which can be derived from the classic Stokes second-order solution. The method relies upon two fundamental assumptions: narrow-band spectrum and second order non-linearity. As a consequence of the last assumption, theoretical limits of the model should also be considered when applying the method. These may be expressed in terms of the generalised Ursell parameter or the "significant slope".

Let  $S_{\eta}(f)$  be a non-linear spectrum, as our spectrum measured at any location in the wave flume. Using the well-known Wiener-Khinchine relation (Bendat and Piersol, 1971) we can write:

$$B_{\eta}(\tau) = \int_0^{\infty} S_{\eta}(f) \cos(2\pi f\tau) df \quad (1)$$

Starting from Stokes' theory, it may be shown that the autocorrelation function  $B_{\eta}(\tau)$  of surface elevation may be written as:

$$B_{\eta}(\tau) = B_{\eta}^{(1)}(\tau) + B_{\eta}^{(2)}(\tau) \quad (2)$$

where  $B_{\eta}^{(1)}(\tau)$  and  $B_{\eta}^{(2)}(\tau)$  are respectively the first- and the second-order autocorrelation functions.

Second order contribution  $B_{\eta}^{(2)}(\tau)$  may in turn be expressed as function of first-order contribution  $B_{\eta}^{(1)}(\tau)$  as:

$$B_{\eta}^{(2)}(\tau) = 8 [f_2(k_0, h)]^2 [B_{\eta}^{(1)}(\tau)]^2 \quad (3)$$

where  $f_2(k_0, h)$  is a function of depth  $h$  and wave number  $k_0$  (relative to the peak frequency), equal to:

$$f_2(k_0, h) = \frac{k_0}{4} \left[ \frac{3}{\tanh^3(k_0 h)} - \frac{1}{\tanh(k_0 h)} \right] \tag{4}$$

Substituting (3) into (2) allows us to calculate  $B_\eta^{(1)}(\tau)$  as:

$$B_\eta^{(1)}(\tau) = \frac{-1 + \sqrt{1 + 32 [f_2(k_0, h)]^2 B_\eta(\tau)}}{16 [f_2(k_0, h)]^2} \tag{5}$$

while  $B_\eta^{(2)}(\tau)$  may then be obtained from (3).

Lastly, first- ( $S_\eta^{(1)}(f)$ ) and second- order ( $S_\eta^{(2)}(f)$ ) spectra may easily be obtained from corresponding autocorrelation functions  $B_\eta^{(1)}(\tau)$  and  $B_\eta^{(2)}(\tau)$  again using Wiener-Khintchine's relations.

Application of theoretical model: comparisons and discussion

Spectral wave transformations obtained in the laboratory were interpreted and compared with the results of above non-linear theory, by calculating first and second-order contributions for measured spectra.

As examples, measured and calculated spectra for tests 2 ( $h = 40$  cm,  $H_{m_0} = 7.9$  cm,  $T_p = 1.28$  s) and 5 ( $h = 50$  cm,  $H_{m_0} = 9.4$  cm,  $T_p = 1.28$  s) are shown in Figs. 8 and 9 for gauges 1, 6, 8 and 12. For better evidence of linear and second-order contributions, spectral densities are drawn on both linear and logarithmic scales.

Considering first the results for test 2, these show the very small contributions of second-order components for the offshore data (gauge 1).

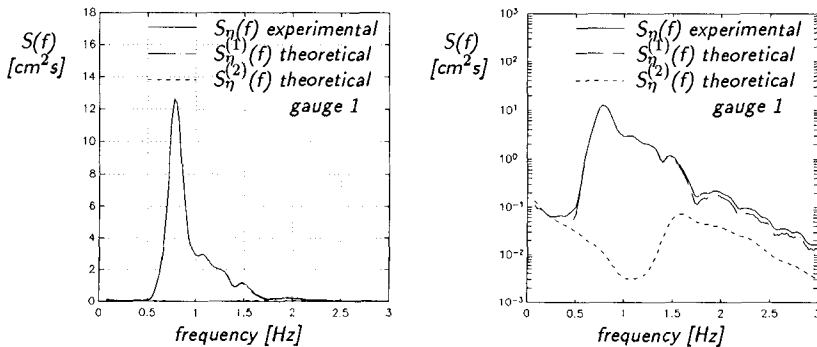


Fig. 8a – Example of wave spectra computed during test 2 (gauge 1) expressed in linear (left) and logarithmic scale (right).

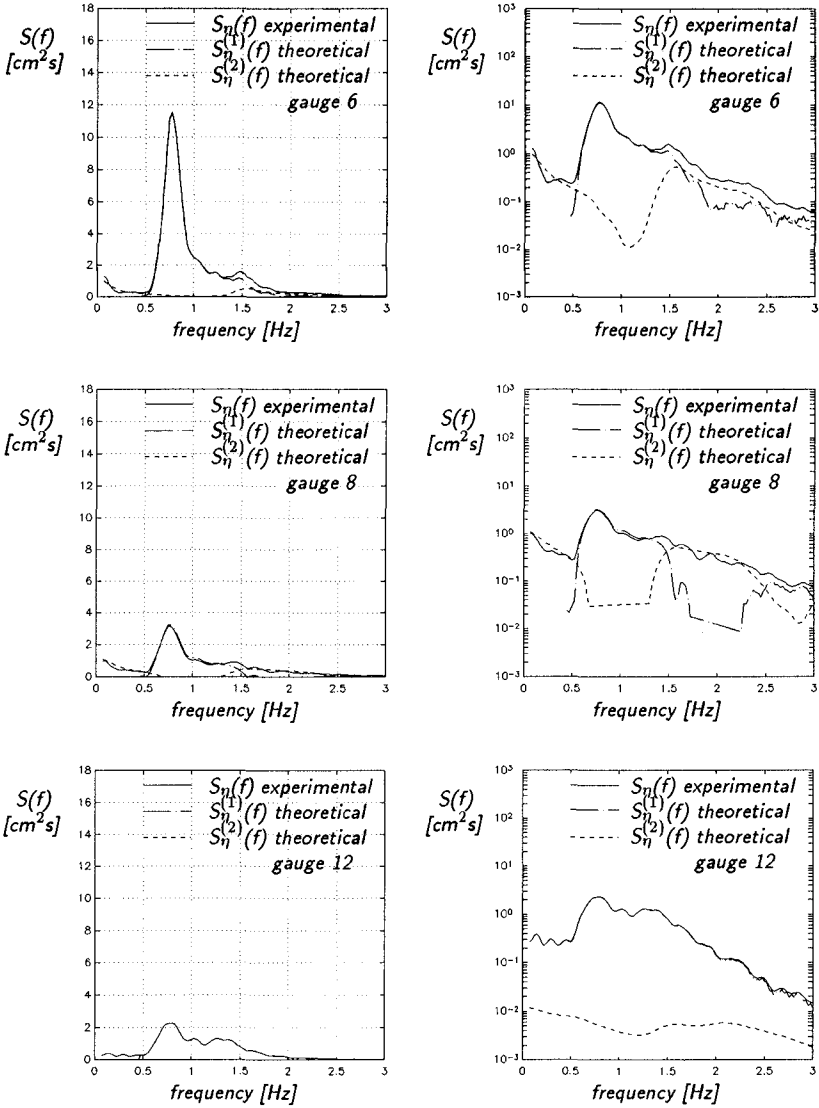


Fig. 8b – Example of wave spectra computed during test 2 (gauges 6, 8 and 12) expressed in linear (left) and logarithmic scale (right).

These become important with decreasing depths, as indicated by the results for gauge 6 (at the end of the offshore slope, near the top of the bar, just before intensive breaking occurs). In this case, second-order components at low and high frequencies are evident and may be predicted accurately by the

analytical model.

For gauge 8, the results do not appear very convincing, if only because the second-order components are in some cases greater than measured spectra. At the position of this gauge (above the top of the barrier, shoreside) intensive breaking occurs, and the measured spectrum is rather wide and therefore not suitable for analytic treatment, since this requires narrow banded spectra.

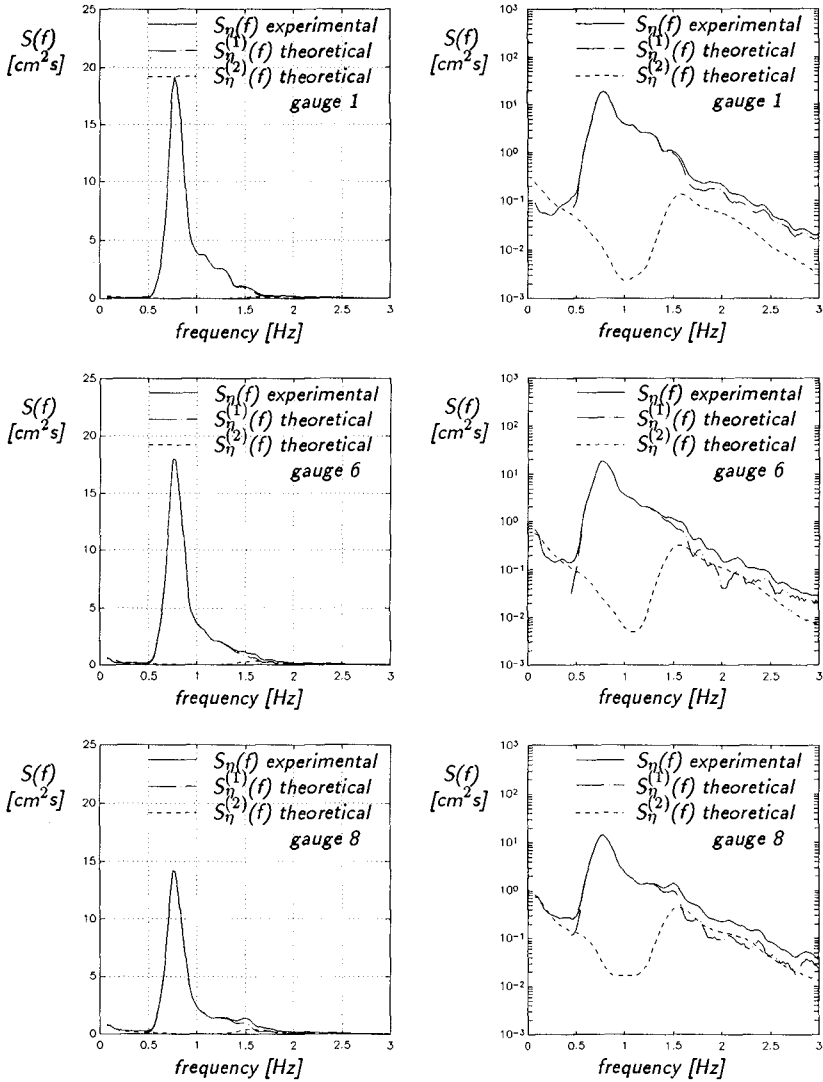


Fig. 9a – Example of wave spectra computed during test 2 (gauges 1, 6, and 8) expressed in linear (left) and logarithmic scale (right).

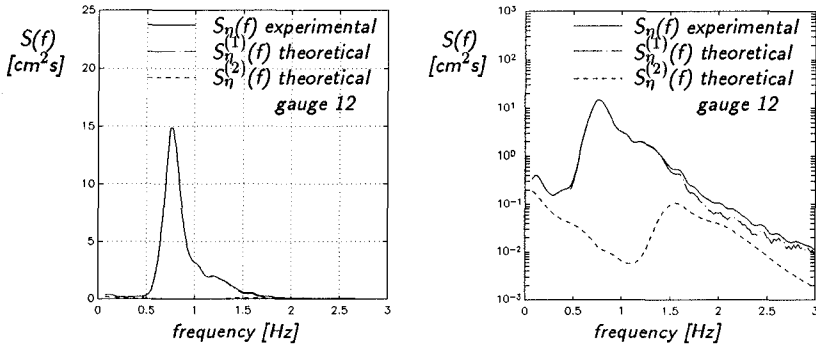


Fig. 9b – Example of wave spectra computed during test 2 (gauges 12) expressed in linear (left) and logarithmic scale (right).

Nevertheless, low frequency components may still be predicted quite well by the model.

Lastly, the spectrum measured at gauge 12 (shoreside of the bar) is quite broad and far beyond the applicability of the method; calculated second-order components are very small and not very meaningful.

For test 5 ( $h = 50$  cm,  $H_{m0} = 9.4$  cm,  $T_p = 1.28$  s) analytical results also appear satisfactory for shoreside gauges such as gauge 8. This is ascribable, in this case, to less intense breaking occurring above the bar (due to greater depths over it); measured wave spectra are still rather narrow and non-linear effects still pronounced.

In this case too, non-linearities become very small, due to greater water depths, for gauges located shoreside of the bar and therefore, again, the method cannot be properly applied.

### Summary and conclusions

Transformations of random waves over a submerged bar are investigated in this paper.

In particular, experimental results are analysed through zero-crossing analysis (including separation of short and long waves) and spectral analysis. In this regard, some features of the evolution of variance spectra above the bar were observed and the importance of non-linear effects and breaking on spectral transformations are highlighted and discussed.

Modified zero-crossing analysis allowed us to reveal some aspects of long wave behaviour over the submerged bar. A new and interesting problem observed during the experiments was the possibility of long waves resonances between the spending beach and the bar.

The influence of flume seiches on this phenomenon will be more fully investigated with new experiments to be carried in the near future using a longer flume. In these experiments, a new absorbing system recently installed on the flume will allow to investigate the influence of paddle re-reflection of waves on the observed phenomena.

A second order analytical method was applied to the data in order to

interpret non-linear transformations of spectra. As regards the procedure applied, which separates first- and second-order components for the measured spectra, the analytical method used seems conveniently applicable to describe non-linear effects, as long as breaking phenomena are not too intense.

### Acknowledgements

This work was undertaken within the framework of the MAST G6 Coastal Morphodynamics research programme. It was funded by the Commission of the European Communities, Directorate General for Science, Research and Development under contract no. 0035C.

The helpful comments received during this work from Mr M.W. Dingemans of Delft Hydraulics are gratefully acknowledged.

### References

- Battjes J.A. and Beji S. (1992). *Spectral evolution in breaking waves propagating over a shoal*. 23rd International Conference on Coastal Engineering, Venice.
- Beji S., Ohyama T., Battjes J.A. and Nadaoka K. (1992). *An experimental verification of a numerical model for nonlinear random waves*. 23rd International Conference on Coastal Engineering, Venice.
- Bendat J.S. and Piersol A.G. (1971). *Random Data: Analysis and Measurement Procedures*. Wiley - Interscience, New York.
- Brocchini, M., Cherubini, P. and Iovenitti, L. (1991). *An extension of a Boussinesq type model to the surf zone*. Extended abstract, MAST G-6 Morphodynamics Mid-Term Workshop, Edinburgh.
- Goda Y. and Suzuki, Y. (1976). *Estimation of incident and reflected waves in random wave experiments*. Proc. 15th Int. Conf. on Coastal Eng., ASCE, 828-845.
- Liberatore, G. and Petti M. (1991). *Random wave transformation over a submerged bar*. Extended abstract, MAST G-6 Morphodynamics Mid-Term Workshop, Edinburgh.
- Petti M. (1988). *Second Order Analysis of Shallow-Water Wave Spectra*, II Nuovo Cimento, Vol. 11 C, N. 5-6.
- Petti, M. (1991). *On the separation of second order components for non-linear wave spectra*, Proc. 2nd Int. Conf. on Computer Modelling in Ocean Engineering, Barcelona.
- Rojanakamthorn, S., Isobe, M. and Watanabe, A. (1990). *Modelling of wave transformation on submerged breakwater*. Proc. 22nd International Conference on Coastal Engineering, ASCE, 1061-1073.
- Schäffer, H.A., Deigaard, R. and Madsen P.A. (1991). *Incorporation of wave breaking in a Boussinesq model*. Extended abstract, MAST G-6 Morphodynamics Mid-Term Workshop, Edinburgh.
- Smith E.R. and Kraus N. C. (1992). *Laboratory study of wave transformation on barred beach profiles*. 23rd International Conference on Coastal Engineering, Venice.
- Thorkilsen, M., Rosing N. and Schäffer, H.A., (1991). *Experiments on waves breaking over a bar*. Extended abstract, MAST G-6 Morphodynamics Mid-Term Workshop, Edinburgh.